CONF-820338--3 Pt2 Rev1

MASTER

UCRL- 87378, Part II, Rev. I
PREPRINT

UCRL--87378 Pt. 2-Rev. 1

DE82 019116

RECENT U.S. TARGET-PHYSICS-RELATED RESEARCH IN HEAVY-ION INERTIAL FUSION: SIMULATIONS FOR TAMPED TARGETS AND FOR DISK EXPERIMENTS IN ACCELERATOR TEST FACILITIES

James W-K. Mark

Lawrence Livermore National Laboratory

This is Part II of the invited survey
paper presented at the
1982 GSI Symposium on Accelerator Aspects of
Heavy-Ion Fusion, March 29, 1982,
Darmstadt, West Germany

June 24, 1982

UCRL-87378
Part II, Rev 1

RECENT U.S. TARGET PHYSICS RELATED RESEARCH IN HEAVY-ION INERTIAL FUSION: SIMULATIONS FOR TAMPED TARGETS AND FOR DISK EXPERIMENTS IN ACCELERATOR TEST FACILITIES

James W-K. Mark

Lawrence Livermore National Laboratory

This is Part II of the invited survey
paper presented at the
1982 GSI Symposium on Accelerator Aspects of
Heavy-Ion Fusion, March 29, 1982,
Darmstadt; West Germany

March 22, 1982

ABSTRACT

Within the last few years, there have also appeared in the Heavy-Ion Fusion literature several studies of targets which have outer tampers. One-dimensional simulations indicate higher target gains with a judicious amount of tamping. But for these targets, a full investigation has not been carried through in regards to conservative criteria for fluid instabilities as well as reasonable imperfections in target fabrication and illumination symmetry which all affect target ignition and burn. Comparisons of these results with the gain survey of Part I would have to be performed with care.

Our calculations suggest that experiments relating to high temperature disk heating, as well as beam deposition, focusing and transport can be performed within the context of current design proposals for accelerator test-facilities. Since the test-facilities have lower ion kinetic energy and beam pulse power as compared to reactor drivers, we achieve high-beam intensities at the focal spot by using short focal distance and properly designed beam optics. In this regard, the low beam emittance of suggested multi-beam designs is very useful. Possibly even higher focal spot brightness could be obtained by "plasma lenses" which involve external fields on the beam which is stripped to a higher charge-state by passing through a plasma cell. Preliminary results sugg ᵗ that beam brightnesses $\sim 10^{13}$-10^{14} W/cm^2 are achievable. Given these brightnesses, deposition experiments with heating of disks to greater than a million degrees Kelvin (86 eV) are expected. We might also expect as much as 1-3 kA of incident ion current on these disks with beam brightnesses almost comparable to that of reactor targets. Thus, if

"Work performed under the auspices of the U.S. Department of Energy by the Lawrence Livermore Laboratory under contract number W-7405-ENG-48."

any anomalous plasma effects on deposition exist, the conditions should be available for discovering some of them. We should also note that these deposition experiments have low ion kinetic energy per nucleon. About 4-5 MeV/nucleon is appropriate if lighter ions such as sodium were used. But for lighter ions, unexpected plasma effects in deposition might be more readily noticed because heavy-ion beams are more "stiff."

VII. SOME RECENT NUMERICAL SIMULATIONS OF TAMPED TARGETS

In addition to the survey of best estimate target gains described in the preceeding sections, there has also been work in the last few years on individual designs where the goals are: (1) to introduce modifications some of which might eventually prove to increase target gain or improve the physics models; (2) to investigate simpler and low gain targets for early experiments or fusion-fission hybrid applications. On the whole, these targets have not been fully investigated in regards to conservative criteria for effects of fluid instabilities as well as reasonable imperfections in target fabrication and illumination symmetry which all affect target ignition and burn. Nor have these designs been pursued to the extent of providing a grid of models for a survey. Therefore, any comparisons with those gain results of Section III would have to be performed with care. Hopefully, further work on these targets in the next few years would fill this gap.

Notable among the first category is the double-shell target with the additional outer tamper [35]. The target's generic shape is shown in Fig. 13. One starts with a solid DT fuel region surrounded by a high-Z pusher. This is isolated from the second shell by a low density gas cushion. The main fuel layer is next, again frozen to allow a density of .21 g/cm^3. A seeded region of DT surrounds the fuel to isolate it from preheat due to the hotter deposition layer. Seeded DT is preferred over a high-Z preheat shield because it reduces instability and mass. The last two layers make up the low-Z deposition layer and high-Z hydro tamper. In all the calculations, the central fuel remained fixed in size and material. The gas cushion density was changed as the pulse shape was varied to regain optimum conditions. However, the biggest variety occurred in the material chosen for the deposition layer and the thickness of the deposition layer and tamper layers.

In one dimensional computer simulations this target exhibits net gain of 260 for 1.7 MJ of 5 GeV U beam at 90 TW beam power. The tamping is particularly effective because an ion has a higher dE/dx in low-Z materials than high-Z. Thus, with more energy per gram deposited in low-Z materials, one would preferentially choose this as the deposition material. Furthermore, for a given shell mass, low-Z shells are thicker and therefore less subject to fluid instabilities. Changing the thickness of the tamper for these targets produced varying results. Figure 14 indicates the change in yield from the 5 and 10 GeV targets as the thickness of the tamper is varied. For the 10 GeV case, the output is relatively insensitive over a broad range of thicknesses. However, the 5 GeV exhibits a rather pronounced peak at .03 g/cm^2 and deteriorates rapidly on either side.

To study this tamping effect further, a larger diameter target was calculated [35] with 5 GeV uranium ions and various amounts of tamper thickness. To see the effect of raising the spot diameter, examples were calculated up to .3 cm focus and the results were plotted in Fig. 15. One notes that below a certain spot size, the effect on gain is minimal, but for large beams, the target behaviour deteriorates badly. Also, some tamping is beneficial in improving the gain.

The possibility of preheat caused by the K and L line emission from the high-Z due to the ion beam stopping was also investigated [35]. Several runs were made to study this: it was found that a source of 60 keV photons equal in strength to 1% of the beam energy and placed uniformly in the high-Z tamper could destroy the target. Using the Bethe formula and calculating the stopping power due to each electron in lead, it was estimated that less than 4% of the beam energy could be converted to L line emission (10-15 keV) and .06% into K line emission (55-65 keV). The above estimates are for a 10 GeV beam and putting this photon source into the 5 GeV target to simulate an upper limit preheat. No changes in yield were observed.

All of the above calculations were performed in one dimension only. Studies of multi-dimensional effects such as symmetry and stability are only in the preliminary stages [35,38], but most certainly will have a negative effect on the target's gains. Another effect that will reduce the gain is mixing of the high-Z shell into both the ignitor and the main fuel. Although the stated gain of 260 had already been reduced by several multipliers in part to account for this mixing, recent studies [39] indicate that the yield may degrade even further, implying that the 260 figure may not be sufficiently conservative. Further work is required to determine the extent of the multi-dimensional effects.

Some additional work continues for the corresponding single-shell tamped target of Ref. [40] (cf. Fig. 16). For example, there is a study [41] of possible preheat due to the production of fast precursors by nuclear interactions between the incident heavy-ions and the outer parts of the target. Their tentative conclusion is that the resultant preheat level is an order of magnitude lower than that which would impair target performance. We also briefly mention here a few improvements in physics modelling which deserve investigation firstly for these single-shell tamped targets: (1) The cryogenic DT shell should be in reality be in equilibrium with some DT vapor; introduction of this vapor at 10^{-6} to 10^{-5} g/cm^3 in the central regions helps ignition conditions for these targets possibly by guaranteeing a small central hot spot; (2) Heavy-ions are found to deposit less of its energy in the high-Z outer tamper than previously assumed because it takes a finite time for the incident ion to reach equilibrium charge [42].

For application to fusion-fission hybrid reactors, target gains 10-20 might be sufficient. The use of cryogenic single-shell targets at 1-2 MJ is certainly adequate. For this purpose and for the purpose of initial experiments in Heavy-Ion Fusion, there have been investigations of volume ignition targets (cf. Fig. 17). Volume ignition targets tend to have less physics uncertainties and are easier to fabricate because they do not require propagating burn nor cryogenics. A recent study [43,44] in the Heavy-Ion literature discusses simple single-shell cases of low density DT gas inside a gold tamper. They obtained a maximum 1-D gain of 11 ror 1 MJ of 6.4 GeV Xe at 150 TW. We estimate that pulse shaping and somewhat more fuel should allow 1-D gains of 30-50 without exceeding 240 TW of driving power. A comprehensive study of stability and symmetry considerations (including beam entrance angle effects and reasonable fabrication imperfections) have yet to be carried through to completion (but cf. [45]). It is not clear that conservative target gains could be as high as 10 for these latter targets with the present requirements on peak power, because of possible mixing of high-Z tamper material into the fuel. A similar target with low-Z deposition material between tamper and fuel should give better performance. It is being studied.

VIII. SOME PROPOSED DISK HEATING, FOCUSING AND BEAM TRANSPORT EXPERIMENTS FOR ACCELERATOR TEST FACILITIES

For reactor targets in ion-beam inertial fusion, required beam brightnesses I range from some 10^{13}-10^{15} W/cm^2 (10^1-10^3 TW/cm^2, 1 TW=10^{12}W) where the lower numbers are possible only for relatively short ion-ranges (cf. Figs. 3-4). Also specific energy deposition $w = E/\pi r^2 R \sim$ 20-50 MJ/g must be attained. As part of the technology development program for HIF, there are plans to demonstrate with multi-gap accelerators that significant beam brightnesses and specific energy deposition can be achieved (cf. R. Bangerter's talk, this conference).

If we assume that funding would allow construction of a test facility accelerating a few kilojoules of ions to say 100 MeV and several kiloamps of current, then a preliminary estimate suggests that the emergent beams from some accelerator test-facilities could already be ballistically focused to an intensity comparable to 10^{13} W/cm^2 (100 kA/cm^2). Some of our numerical examples [46-48] are motivated by the parameters of an existing conceptual design proposal [49] for a multi-beam [28] induction linear accelerator test-facility. Focusing and increasing beam intensity in this case is facilitated by: (1) the low normalized emittance of $\sim$ (1-5) x 10^{-2} mrad-cm per beamlet; (2) the use of Na ions; (3) compression of the beam pulse and (4) by the fact that the intensity increases very rapidly with decreasing focal distance due to the decrease in spot radius consistent with space charge effects. One method of corroborating the achieved beam brightness and specific energy deposition is to measure the temperature of disks heated by the beams. This is one reason behind rephrasing the basic objective as a high temperature experiment (abbrev. HTE, cf. Bangerter, this conference).

A simple model of the disk heating was given in [50] where the peak temperature was determined by a balance of beam power input versus heat loss while the time scale and pulse energy was determined by the need to heat to that temperature. This peak temperature measures both beam brightness and specific energy deposition.

A few details of the numerical simulation of disk heating in one such proposed experiment are given with the help of Figs. 18-23. In particular, Fig. 18 shows the configuration, in which the incident beam is deposited onto low-Z "felt-metal". Firstly, a small hole (in this case extreme $\sim$ 0.34 mm diameter) is drilled in a disk of heavy material such as lead. This hole is subsequently filled with a low-Z metal such as aluminum in low density "felt-metal" form. The heavier lead prevents transverse conversion to hydrodynamic motions while use of low density material (say $\rho \sim 0.15$ gm/cm^3) reduces (actually delays) the conversion into longitudinal hydrodynamic motions. This scheme results in lower hydrodynamic losses and maximizes the internal temperature and duration of peak temperature of the material used for beam heating experiments. Also, the internal temperature of the material is more readily observable and measureable.

The numerical grid of a LASNEX [20] calculation after 2 nanoseconds (near time of peak temperature) is drawn in Fig. 19. About 3 kJ of sodium ions at 100 MeV and 0.3 TW are used. Actually, by 2 nanoseconds, the peak temperature is reached even though only 0.6 KJ of energy is deposited. Subsequently, the disk disintergrates even with care taken to delay hydrodynamic losses. A peak rather than an asymptotic temperature is due to subsequent hydrodynamic disassembly in the longitudual direction. The time variation of disk temperatures at points near the front (where beam enters the disk) is shown in Fig. 20. Figure 21 further illustrates the distribution of the internal temperature across the disk; the several curves are different cuts across the beam deposition material. The rate of energy lost from the front of the disk is given in Fig. 22 versus the rate of energy deposited, while Fig. 23 gives the accumulated energy lost and deposited up to that time as a function of time.

If sodium ions were used in this test-facility instead of a heavier ion such as thallium, a gain in beam power by roughly the square root of the inverse mass ratio is obtained. Unlike reactor drivers with 5-20 GeV ions, there is little penalty to pay in terms of ion range when lighter ions are used for a 100 MeV test-facility.

The above example assumes 3.3×10^{14} W/cm^2. But in order to reach a million degrees Kelvin (86 eV, comparable to ablator temperatures), it is sufficient to have $\sim 0.84 \times 10^{13}$ W/cm^2 which can be reached by ~ 0.6 TW of sodium ions focused to spot diameter of ~ 1.5 mm. Preliminary results [46-48] suggest that these numbers could likely be attainable in an early test-facility similar to an existing conceptual design [49]. Figure 24 illustrates observable temperature versus beam brightness or intensity. (As we can see, the million degree plasma might even be attainable with somewhat lower beam brightness.) For each beam brightness point in Fig. 24, the columns of Table 1 give the corresponding beam power, pulse energy E and specific energy deposition $w = E/\pi r^2 R$ required to reach and maintain peak temperatures for the roughly 1-2 ns needed to make measurements. These points are for Na at 100 MeV. If the ion range is too long, then w is small, and if it is too small, the disk expands too fast. Typically $R \sim 5 \times 10^{-3}$ to 1.5×10^{-2} g/cm^2 is acceptable.

It must be emphasized that Fig. 24 and Table 1 are just indicative results. A more detailed experimental design will have to take careful account of effects such as detector response and the angle between disk and detector, as well as whether the detector angular resolution sees partially the lead tamper. Also, if the spot diameters differ significantly from 1 mm or ion range from that of Na at 100 MeV, more calculations are advisable.

Beyond achieving basic milestones in beam brightness and specific energy, it is legitimate to ask whether useful experiments testing beam deposition physics could be performed. If funding for the test facility allows the luxury of accelerating a heavier ion like Rb to about 400 MeV and focus to correspondingly high beam brightnesses, experiments can be performed which will go a long way towards removing any lingering doubts about heavy-ion deposition physics in high temperature matter. But even if we had to use Na ions at 100 MeV the deposition experiments are still likely to be slight improvements (from HIF viewpoint) over light-ion experiments performed by that date. For example, we would be using somewhat heavier ions and it should continue to be useful to perform experiments for the purpose of ruling out concerns such as preheat due to generation of hot-electrons and radiation. The experiments would become more interesting if we could also maximize the current density to also rule out concerns for anomalous plasma effects (cf. Section IXb). Conceivably, the intensities might even reach 3-4 x 10^{14} W/cm^2 (3-4 MA/cm^2) in this test facility if we utilize "plasma lenses" which involve external focusing forces on a beam which is stripped to a high charge-state in a plasma cell.

We have also briefly considered [46] the possibility of using magnetic focusing (with discharge currents and/or external magnets) of a stripped beam in plasma cells to reduce the final focal spot size on target. In these schemes, the many ion beamlets (perhaps partially combined into a smaller number of bunches) are injected into plasma channels in gas cells with pre-existing focusing fields (e.g. the conceptual scheme of Fig. 25). The ions are quickly stripped by the gas, and the resulting stripped beams are focused down by the external field onto a small spot. As an example, we consider a single final beam with an emittance of $\sim$ 0.2 mrad-cm, and an initial beam radius of $\sim$ 1 mm, being injected into a channel with a discharge current density of 1 MA/cm^2. Assuming a charge-state of $Z \sim 9$, the beam is expected to pinch down to 150 microns after propagating a few centimeters. If we have 10 beam bunches with an emittance of 0.063 mrad-cm per bunch, the same external current will lead to a final spot of 80 microns.

More detailed simulations of these effects are being planned. Before the results are known, it may be prudent to add some conservative factors to the above numbers: (1) there may be a distribution of charge-states in the stripped beam and (2) there may be further phase-space dilutions during the process of combining the beamlets. If we assume that only 1/3 of the particles arrive at the correct focal spot because of the spread of charge-states and that the additional phase-space dilutions increase beam emittance by a factor of 2, an initial 0.3 TW of Na beams might be focusable to 180 μ-m radius or smaller reaching $\sim 1.4 \times 10^{14}$ W/cm^2. Of course, one could also consider bringing to bear further external focusing magnets on this beam in the plasma cell. Based on the results of Fig. 24, we therefore feel that disk heating experiments up to 200 eV temperatures might not be impossible. If attained, these are very interesting intensities and temperatures.

For comparison, the 3 MJ Induction Linear Accelerator for 10 GeV ions designed by Lawrence Berkeley Laboratory as an ICF reactor driver can focus 150 TW of ions to a 2.5 mm radius spot, or 7.6×10^{14} W/cm^2. Thus the $>10^{14}$ W/cm^2 goal for the test facility with auxiliary focusing should be close to reactor scale beam brightnesses. Of course, if beam brightness were the only issue, a comparable 3 MJ driver could be designed to optimize it. In order to give a further comparison with the test facility, we might mention that, with some modifications, the 3 MJ driver design might reach a spot of 1.6 mm radius or $<1.9 \times 10^{15}$ W/cm^2 (Ref. [47]). Simulations of self-pinched beam propagation suggest that alternatively a 1.2 mm radius spot might be obtained from the self-pinching effect of a beam propagating into few torr neon gas starting from initial beam radius of 2 mm. Even a 0.7 mm spot of $< 10^{16}$ W/cm^2 might be achievable by using an external discharge current of $\sim$ 35 kA in a configuration similar to Fig. 25.

The proposed test-facility parameters should also permit useful experiments on beam transport considerations such as neutralization. A 2.4 keV electron beam has the necessary longitudinal velocity to travel in parallel with a 100 MeV Na beam. This kinetic energy per electron is quite small in comparison with the electrostatic potential drop of more than 180 kV associated with an unneutralized Na Beam of 3 kA. Extrapolating from results given by a two-dimensional particle-code simulation (using the HIPPO code), we expect that the coinjection of electron beams with transverse temperatures below 1 keV will produce extremely good neutralization, even if the ion beam is subdivided into as many as 50 individual beamlets.

Besides neutralization experiments, the test-facility will also be expected to provide meaningful tests of the scaling laws for other focusing and transport issues, such as emittance growth and focal spot size variations in unneutralized beams.

Thus, with such a proposed test-facility, we could look forward to performing a number of interesting deposition experiments with heating of disks to possibly greater than a million degrees Kelvin (86 eV). Beam focusing and transport experiments are also expected. We could reach as much as 1 to 3 kA of incident ion current on these disks with beam intensities almost comparable to that of reactor targets. Thus, if any anomalous plasma effects on deposition emerge, the conditions should be available for testing some of them. If they exist, such plasma effects might well be more noticeable for intermediate ions such as sodium than for heavy ions; also the < 4-5 MeV/nucleon achievable is still an order of magnitude smaller than the more realistic heavy ion deposition conditions in reactor targets (where relatively classical deposition is expected).

REFERENCES

[38] Gula, W. P., "A Study of the Effects of Non-Spherically Symmetric Ion Beam Deposition on Spherically Symmetric Targets," Los Alamos National Laboratory Report No. LA-UR-91-2725 (1981).

[39] Nuckolls, J., Executive Summary on Target Physics, Lawrence Livermore National Laboratory Laser Program Annual Report (1981).

[40] Bangerter, R. and Meeker, D., "Ion Beam Inertial Fusion Target Design," Lawrence Livermore National Laboratory Report No. UCRL-78474 (1976).

[41] Tabak, M. and Bangerter, R., "Nuclear Interactions of Heavy Ions," Lawrence Livermore National Laboratory Report No. UCRL-87355 (1982).

[42] Bailey, D., Lee, Y. T., and More, R. M., "Ab Initio Calculations of the Charge-State of Fast Heavy-Ion Stopping in a Finite Temperature Target," Lawrence Livermore National Laboratory Laser Program Annual Report 1981, Article 3.5.5 (1981).

[43] Magelssen, G. R. and Gula, W. P., "Heavy-Ion Targets," Los Alamos National Laboratory Report No. LA-UR-80-3256 (1980).

[44] Gula, W. P. and Magelssen, G. R., "Scaling Laws for Simple Heavy-Ion Targets," Los Alamos National Laboratory Report No. LA-UR-81-1849 (1981).

[45] Sacks, R. A., Arnold, R. C., and Magelssen, G. R., "Irradiation Uniformity of Spherical Heavy-Ion Driven ICF Targets," Nuclear Fusion, in press (1982).

[46] Mark, J. W-K., Bangerter, R. O., Fawley, W. M., Yu, S. S., and Judd, D. L., "Some Proposed Disk Heating, Focusing and Beam Transport Experiments for Heavy-Ion Inertial Fusion Test Facilities," Lawrence Livermore National Laboratory Report No. UCRL-86189, Rev. 1 (1982).

[47] Judd, D. L., "Phase-Space Constraints on Induction-Linac Heavy-Ion Inertial-Fusion Ingiters," Univeristy of California, Lawrence Berkeley Laboratory, Report LBL-14038, UC-21 (1982).

[48] Judd, D. L., "Rough Estimates of Focusing Many Beamlets for Spot Heating: Possible Use of Permanent Magnets," University of California, Lawrence Berkeley Laboratory Report HIFAN-189 (1982).

[49] Herrmannsfeldt, W. B., "High Intensity Multi-Megajoule Heavy-Ion Accelerator: A Plan for Research, Design, Development and Demonstration," Lawrence Berkeley Laboratory, Report HIFAN-158 (1980).

[50] Mark, J. W-K., Bangerter, R. O., Fawley, W. M., Yu, S. S., and Wang, T-S. F., "Some Proposed Disk Heating and Beam Transport Experiments for Heavy-Ion Inertial Fusion Test Facilities," Proceedings of the 4th International Topical Conference on High Power Electron and Ion-Beam Research and Technology, Palaiseau, France (1981).

Table 1. Required Beam Brightness, Power, Energy and Specific Energy at Focal Spot for Each point on Fig. 24.

Brightness ([illegible] m^2)	4.2	8.5	9.5	17.0	22.0	34.0	38.0	44.0	88.0	175.0	330.0
Power (TW)	0.075	0.15	0.3	0.3	0.075	0.6	0.3	0.15	0.3	0.6	0.3
Energy (kJ)	0.8	1.4	2.4	1.8	0.7	6.0	2.7	1.1	1.8	3.0	0.9
$w = E/\pi r^2 R$ (MJ/g)	6	9	9	12	24	41	41	39	63	105	119
Temperature (eV)	72	92	100	111	115	129	131	132	155	188	225

FIGURE CAPTIONS

Fig. 13. Target geometry used in 1-D study of the cryogenic double-shell tamped target.

Fig. 14. Gain versus tamper thickness for 5 and 10 GeV beams for the target of Fig. 13.

Fig. 15. Gain versus tamper thickness and spot size for the target of Fig. 13.

Fig. 16. The cryogenic single-shell tamped target for heavy-ions.

Fig. 17. Generic targets with volume ignition and with propagating burn.

Fig. 18. An appropriate configuration for disk-experiments using heavy ion beams from accelerator test facilities.

Fig. 19. Further illustrates the numberical grid after 2 ns.

Fig. 20. A plot of the disk temperature reached as a function of time for a point near the front of the disk.

Fig. 21. This plots internal temperature as a function of positions across the depth of the disk and at a tie of Fig. 2 ns. The different curves are for several radial positions.

Fig. 22. Plot of rate of energy lost from front of disk (curve a) versus time as compared to rate of energy deposition given by curve d.

Fig. 23. Same as Fig. 5 except that the total enrgy lost is plotted (curve a from front; durve d energy deposited by beam).

Fig. 24. Plot of observable disk temperature versus beam brightness or intensity at focal spot.

Fig. 25. Schematic of supplementary focusing using stripped beam in external magnetic field.

TARGET GEOMETRY USED IN 1-D STUDY OF DOUBLE-SHELL TAMPED TARGET

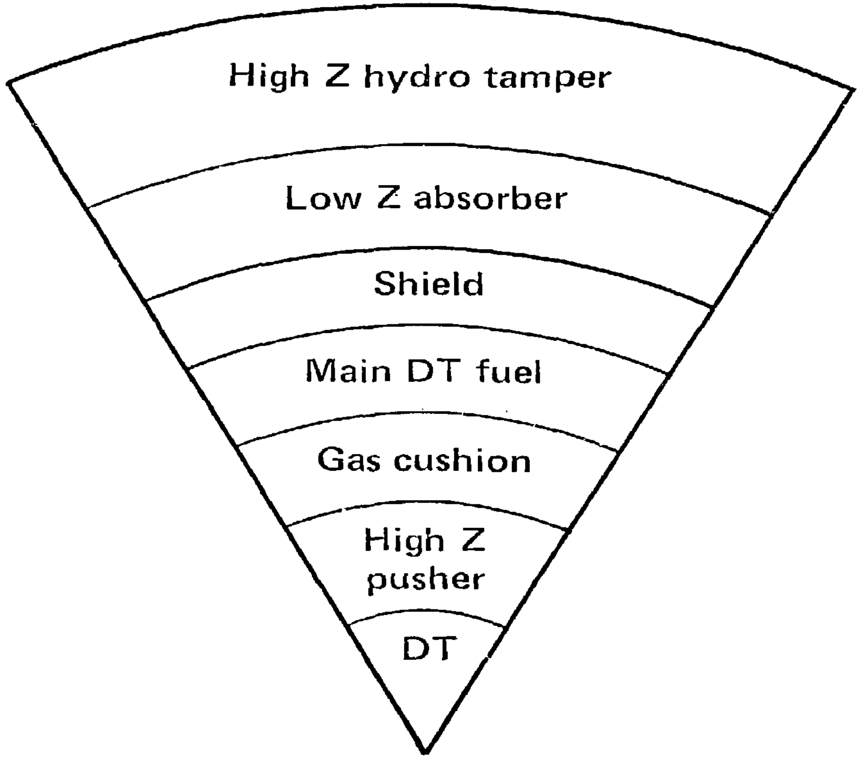

Fig. 13

50-60-0382-1077

GAIN vs TAMPER THICKNESS FOR 5 AND 10 GeV BEAMS AND FOR DOUBLE-SHELL TAMPED TARGET

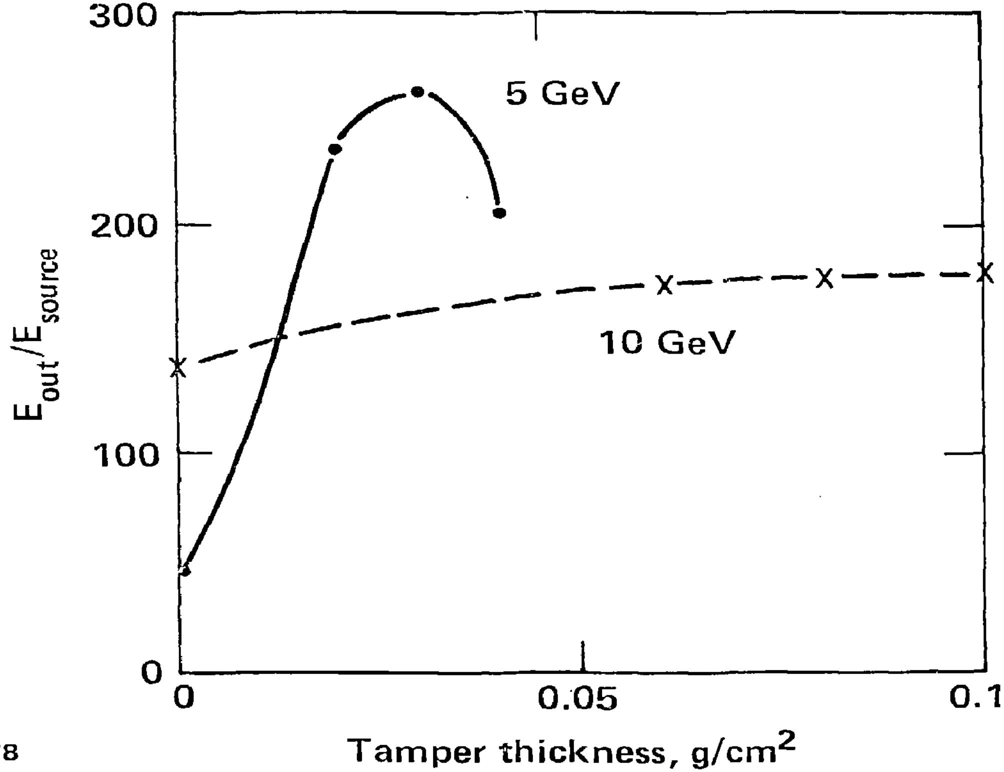

50-60-0382-1078

Fig. 14

GAIN vs TAMPER THICKNESS AND SPOT SIZE FOR DOUBLE-SHELL TAMPED TARGET

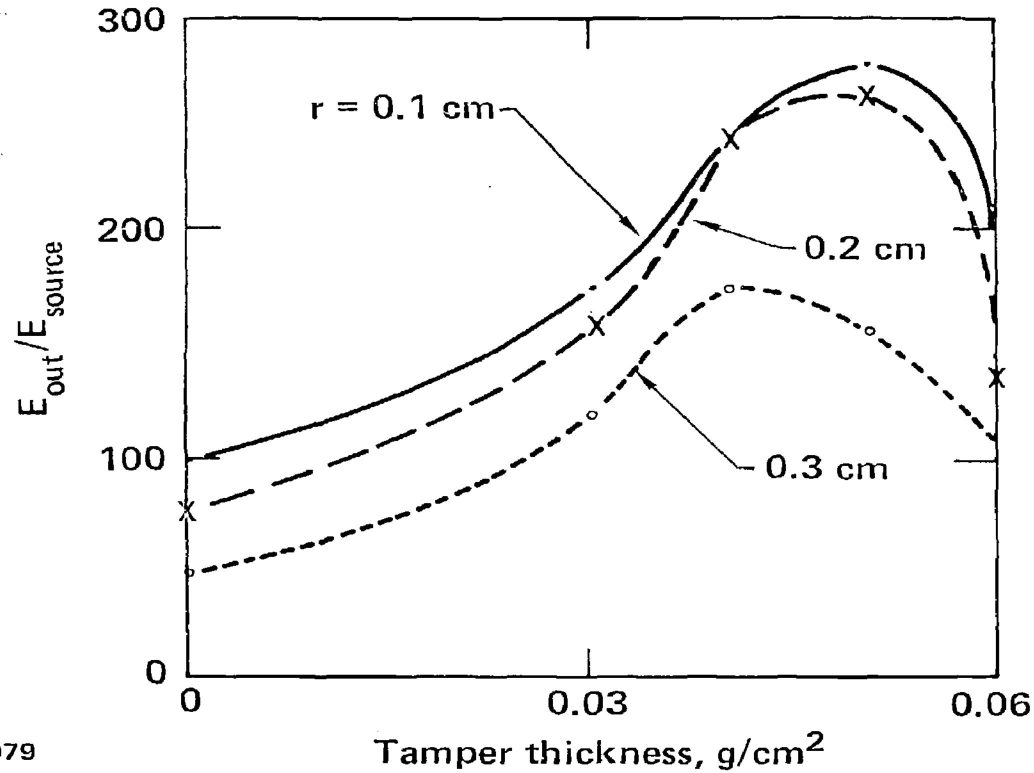

50-60-0382-1079

Fig. 15

A TAMPED ION BEAM TARGET CONFINES GASES AND IMPROVES EFFICIENCY OF IMPLOSION

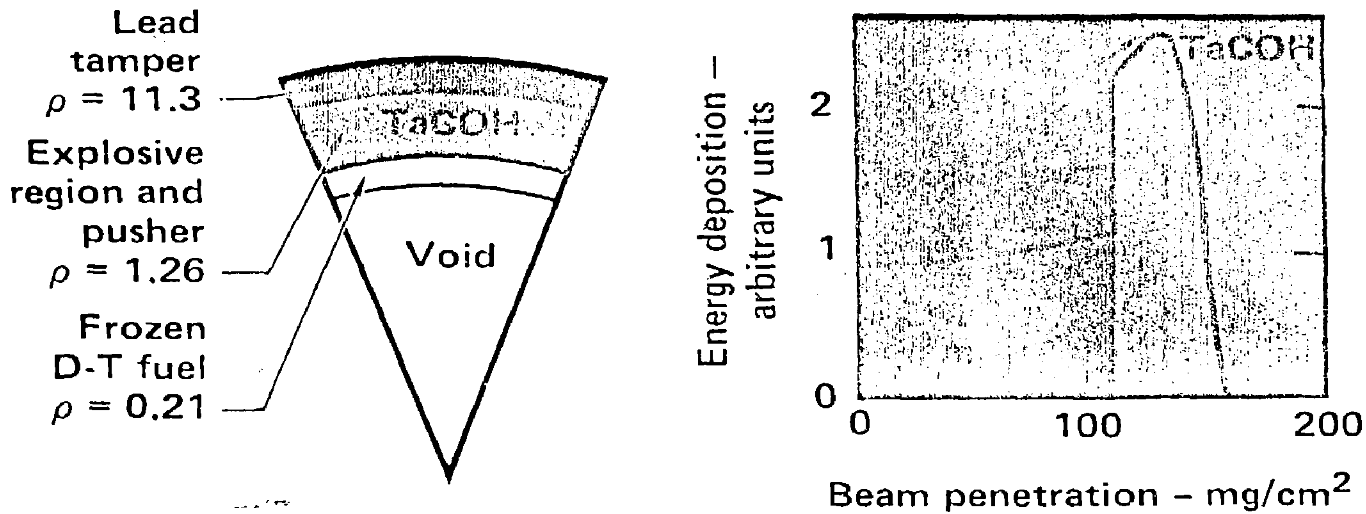

Fig. 16

50-60-0981-3052

SEVERAL TYPES OF TARGETS HAVE BEEN STUDIED

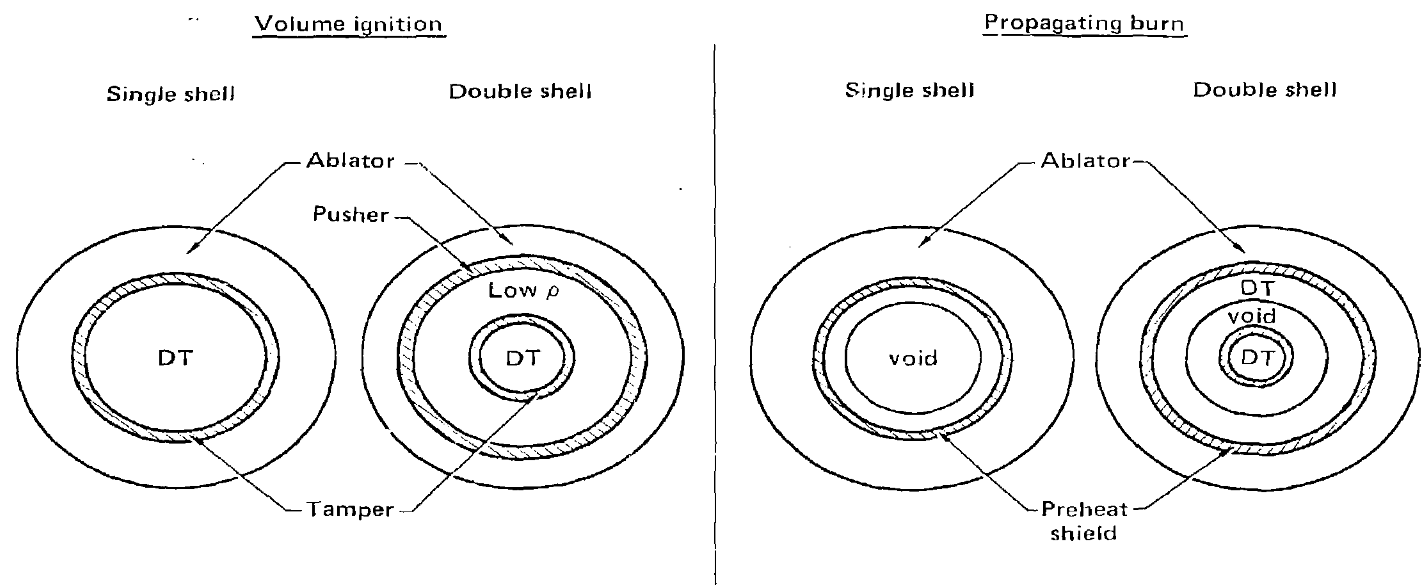

Other targets are possible

Fig. 17

50-60-0881-2143

LOW DENSITY AND LEAD TAMPER MAXIMIZES TEMPERATURE OF DEPOSITION MATERIAL HEATED BY IONS

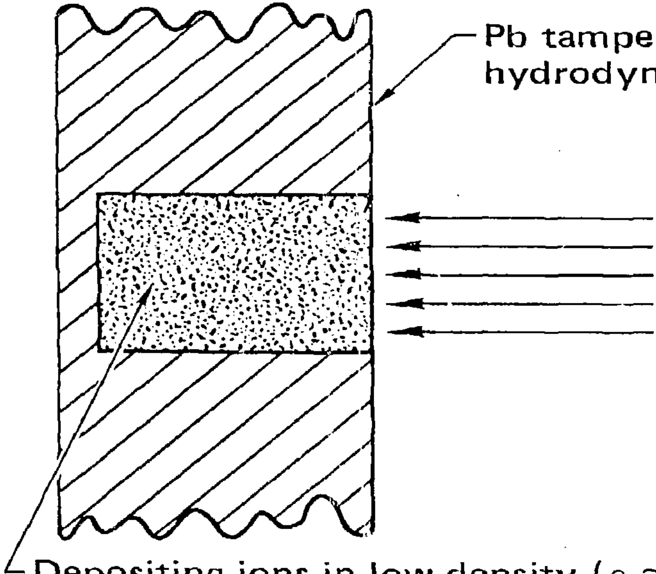

Depositing ions in low density ($\rho \sim 0.15$ gm/cm^3) material reduces conversion to longitudinal hydrodynamic motion and ensures that the internal temperature can be readily observed

Fig. 18

50-60-0681-1606

2/82

NUMERICAL GRID SHOWING PENETRATION OF BEAM IONS INTO DEPOSITION MATERIAL (AT 2 ns)

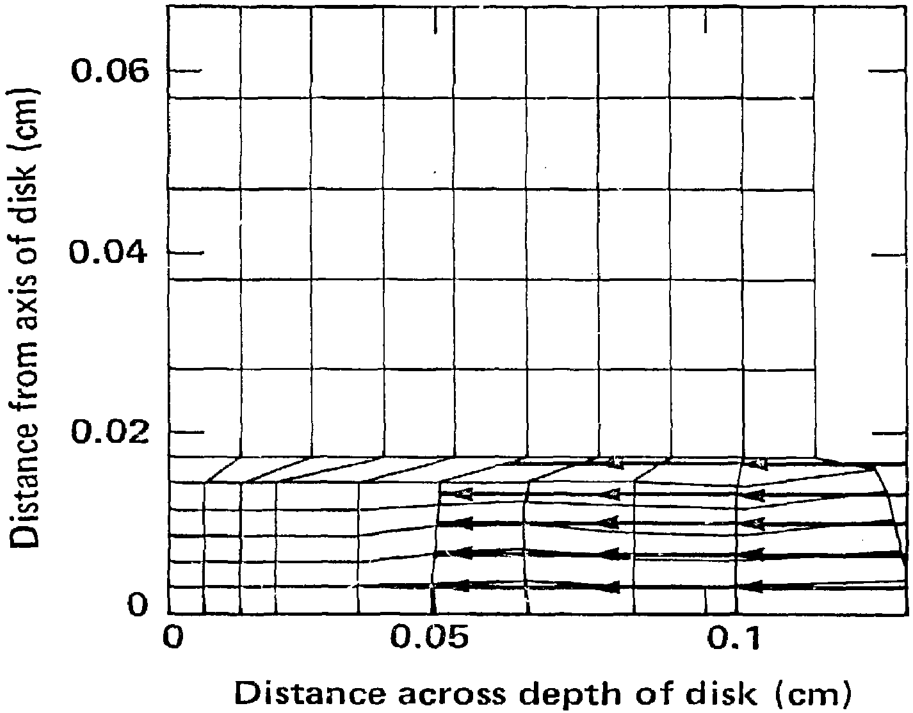

Fig. 19

50-60-0681-1604

Fig. 20

DISK TEMPERATURE VERSUS TIME AS SEEN FROM SIDE OF DISK WHERE BEAM ENTERS

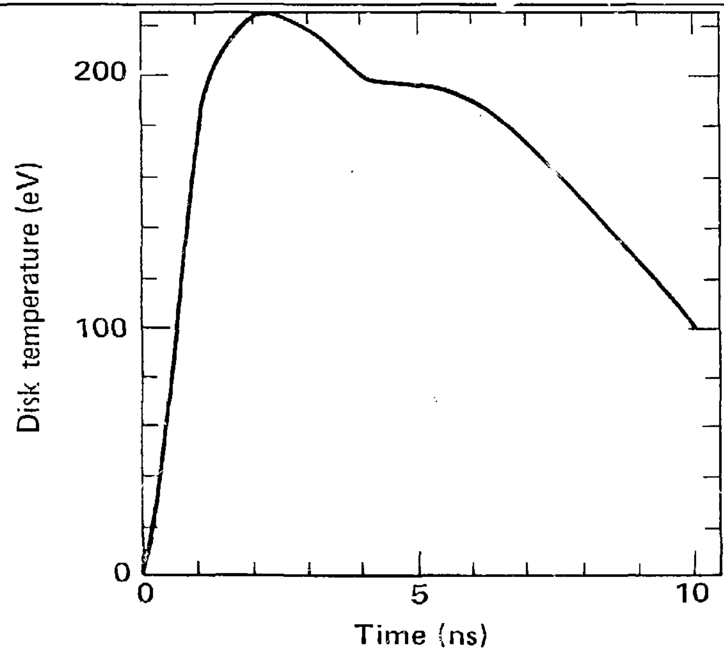

50-60-0681-1600

2/82

Fig. 21

INTERNAL TEMPERATURE ACROSS DEPOSITION MATERIAL OF DISK (AT 2 ns)

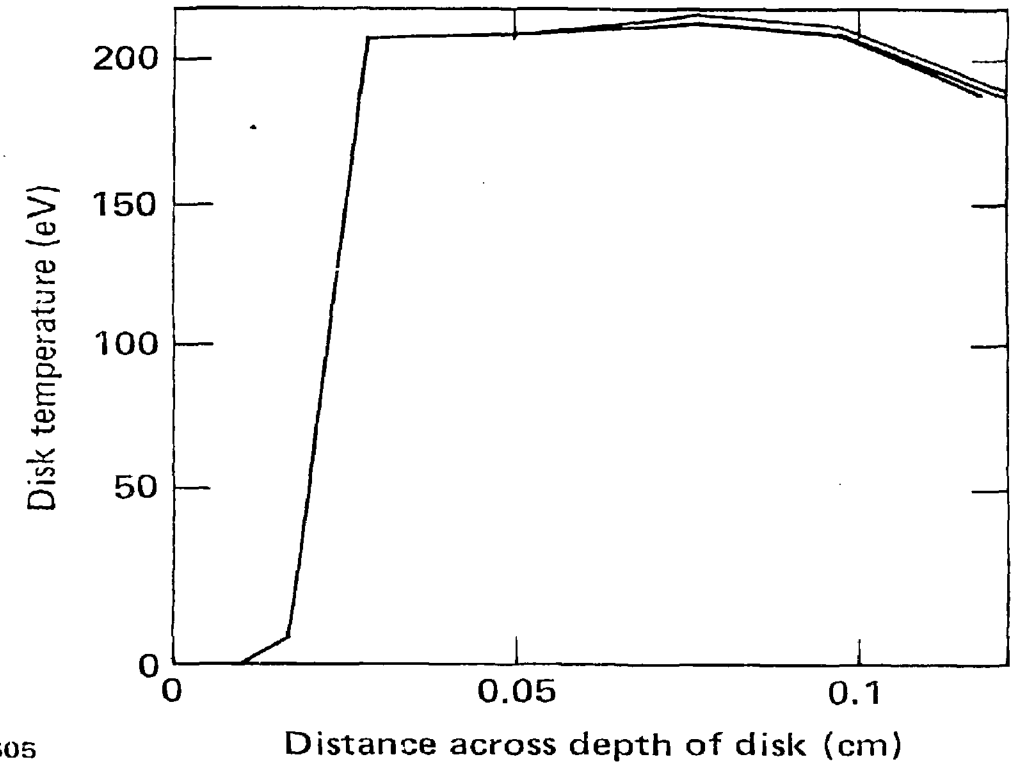

RATE OF ENERGY LOST FROM DISK (SOLID CURVE) VERSUS TIME IS COMPARED WITH RATE OF ENERGY DEPOSITION BY ION BEAM (DASHED CURVE)

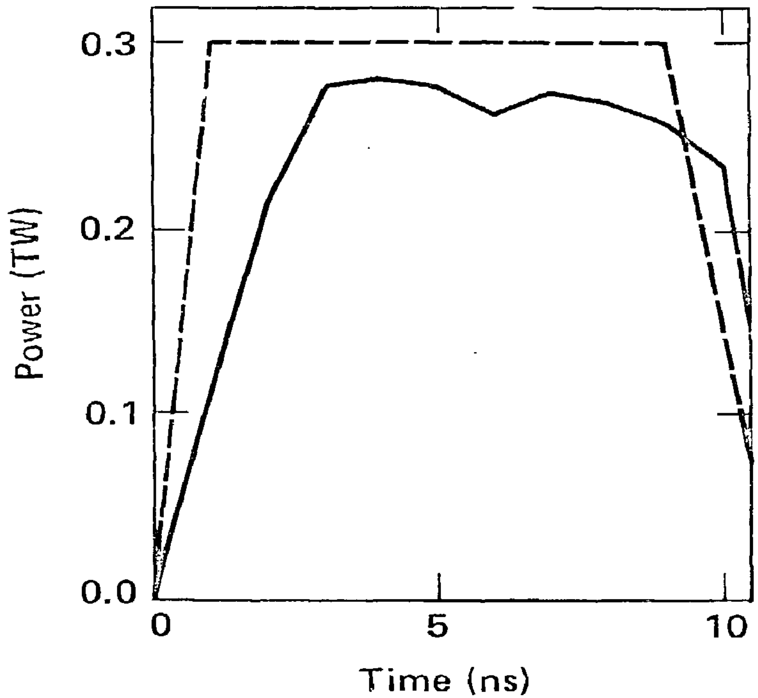

Fig. 22

50-60-0681-1603

2/82

TOTAL ENERGY LOST (SOLID CURVE) VERSUS TIME IS COMPARED WITH ENERGY DEPOSITED BY ION BEAM (DASHED CURVE)

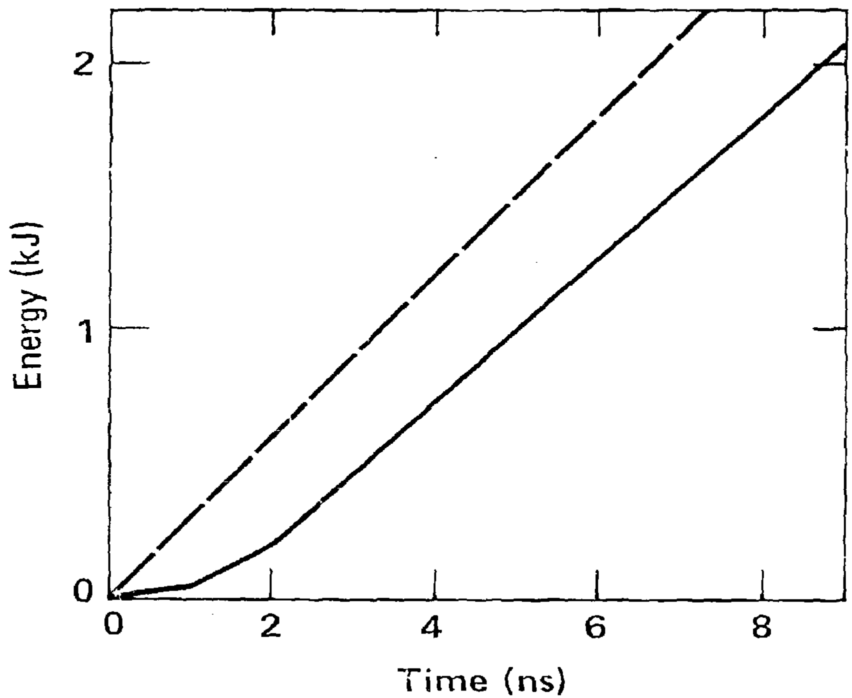

Fig. 23

50-60-0681-1602

2/82

Fig. 24

OBSERVABLE TEMPERATURE OF DISK VERSUS FOCAL SPOT BRIGHTNESS OF INCIDENT ION BEAM

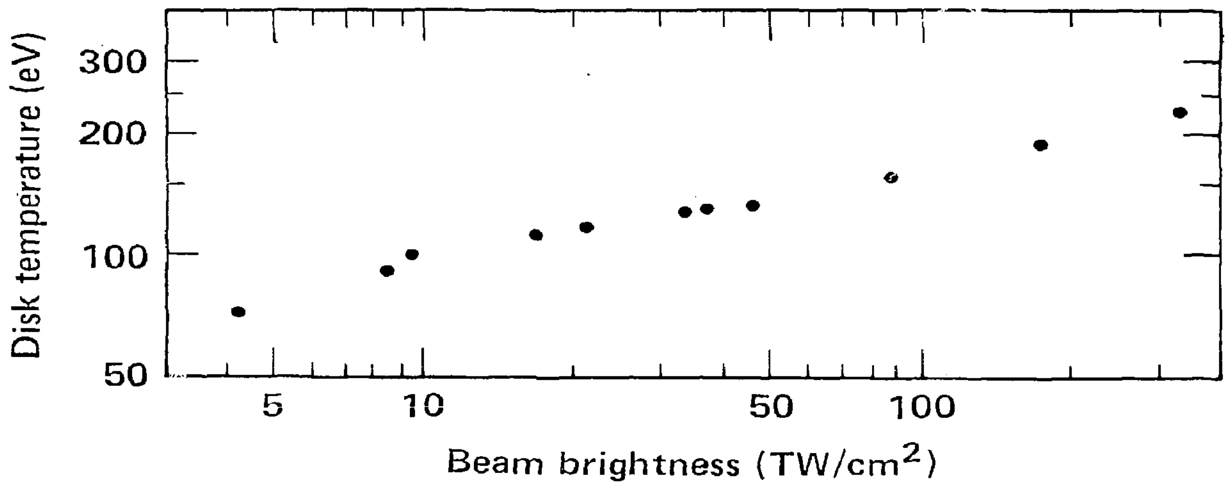

SCHEMATIC OF SUPPLEMENTARY FOCUSING PROCESS USING STRIPPED BEAM IN EXTERNAL MAGNETIC FIELD OF DISCHARGE CURRENT CHANNEL

Fig. 25

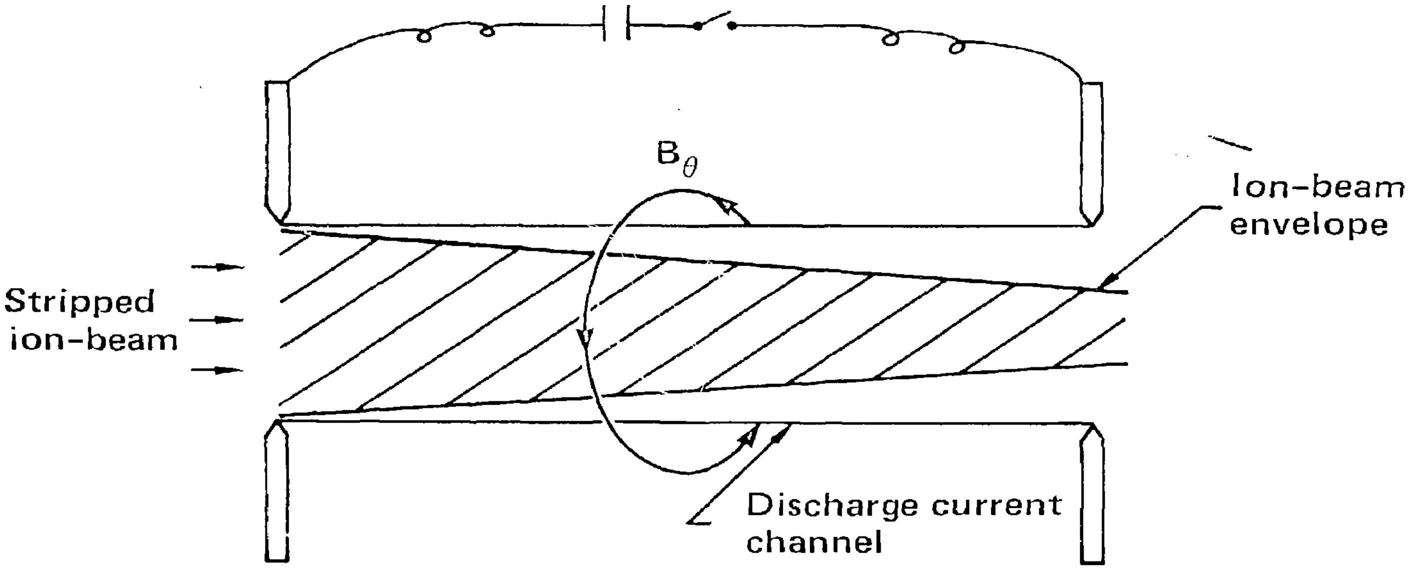

Plasma Cell with Few Torr Neon Gas

50-60-0282-0368